Vietnam Journal of Mechanics, Vol. 46, No. 3 (2024), pp. 253 – 264
DOI: https://doi.org/10.15625/0866-7136/21026

A DESIGN OF TUNED MASS DAMPER WITH PIEZOELECTRIC STACK ENERGY HARVESTER AND TWO-STAGE FORCE AMPLIFICATION FRAME

Nguyen Anh Ngoc[1,*], **Tong Duc Nang**[2], **Vu Anh Tuan**[2], **Nguyen Dong Anh**[3,4], **La Duc Viet**[3,4], **Tran Tuan Anh**[5], **Nguyen Ngoc Linh**[5]
[1]*University of Transport and Communications, Hanoi, Vietnam*
[2]*Hanoi University of Civil Engineering, Hanoi, Vietnam*
[3]*Institute of Mechanics, Vietnam Academy of Science and Technology, Hanoi, Vietnam*
[4]*University of Engineering and Technology, VNU, Vietnam*
[5]*Thuyloi University, Hanoi, Vietnam*
[*]E-mail: nguyenanhngocmxd@utc.edu.vn

Received: 15 March 2024 / Revised: 18 April 2024 / Accepted: 20 May 2024
Published online: 30 June 2024

Abstract. The paper deals with a novel tuned mass damper (TMD) with an energy harvester consisting of a combination of piezo stacks and two-stage force amplification frames connected in series with TMD springs (TMD-2sPSFAFs). The governing equations of 2sPSFAF are established first, followed by those of TMD-2sPSFAF. It will be demonstrated that the reduced order model of the series combination of 2sPSFAF and TMD spring is an equivalent piezo stack energy harvester. Using the optimal results according to the fixed point theory, the conditions for selecting stiffnesses of piezo stacks and TMD spring are obtained. Next, a numerical examination of the electromechanical system reveals that the voltage amplitude curve has a fixed point independent of TMD spring stiffness. Furthermore, an effective stiffness of the TMD spring would be found to ensure that the peaks of mechanical magnification and voltage amplitude curves are of equal heights.

Keywords: tuned mass damper, piezo stack energy harvester, two-stage force amplification frame.

1. INTRODUCTION

Recently, piezoelectric energy harvesting has become a popular subject in vibration energy transmission. This can be attributed to the fact that piezoelectric materials possess a simpler structure and provide a greater energy density compared to other energy

transmission mechanisms such as electrostatics and electromagnetism. Common piezoelectric structure types are (cantilever) and (piezo stack) [1]. The piezo stack is made up of many layers of piezoelectric ceramics mechanically linked together consecutively and interspersed with electrodes. With such structural characteristics, the piezoelectric stack can withstand mechanically the large load, as well as allow the distance between electrodes to be reduced, thereby increasing energy harvesting efficiency compared to a piezoelectric block of the same size [2].

Since the 2010s, the application of piezo stacks in many engineering fields has been widely studied such as shoes [3], pavement [4], suspension systems [5], railways [6], and TMD [7]. However, the stand-alone piezo stack could only harvest a small amount of energy and it is vulnerable to damage without any protection [8]. In order to improve these disadvantages, force amplification frames (FAFs) have been developed as effective auxiliary elements for piezo stacks [9]. The application of piezo stack for TMD and/or dynamic vibration absorber has become a rising interest in the last few years [7, 10, 11]. Such a device is also called the dual-functional one. The working principle of the system is that the vibration energy of the primary structure is transferred partially to the TMD, then a part of the transferred energy is absorbed by the TMD damper, and the other is converted to electrical energy through the piezo stack energy harvester (PSEH). In [7], a damped TMD-PSEH attached to a damped primary structure is studied. The proposed PSEH is attached in series to the TMD spring and is a multiple-row-column piezoelectric stack that can be characterized by an equivalent piezoelectric stack. The optimal design procedure for the PSEH is performed using the available numerical optimization solver. In [10], a system of dynamic vibration absorber integrated with a PSEH (DVA-PSEH) subjected to base excitation is introduced. The mechanical and electrical responses of the electromechanical system are determined by the complex amplitude method, then the numerical simulations are carried out to investigate the characteristics of DVA-PSEH. In the Patent [11], a TMD incorporating piezo stack energy harvesters with two-stage FAFs is proposed. This piezo TMD is denoted as TDM-2sPSFAF. The novelty of the proposed system is the series combination of the TMD springs and 2sPSFAF. The modeling of the series combination of the TMD spring and piezo stack is performed in [12], and the series combination of the TMD spring and the single-stage PSFAF (1sPSFAF) is carried out in [13]. It is shown that those reduced-order models can be presented as equivalent piezo stack energy harvesters. Numerical investigation of the electromechanical system reveals that all mechanical magnification factors and voltage amplitude curves have fixed points independent of damping. Notably, a successful extension of the fixed point theory to TMD-PSEH has recently been performed in [14].

This paper is concerned with a design consideration of TDM-2sPSFAF. Modeling of the electromechanical system and some design conditions derived from the fixed point

theory are implemented in Section 2. Numerical examination is carried out in Section 3. Section 4 contains a summary and conclusions.

2. TUNED MASS DAMPER WITH ENERGY HARVESTER OF PIEZOELECTRIC STACK AND FORCE AMPLIFICATION FRAME

2.1. Modeling two-stage PSFAF

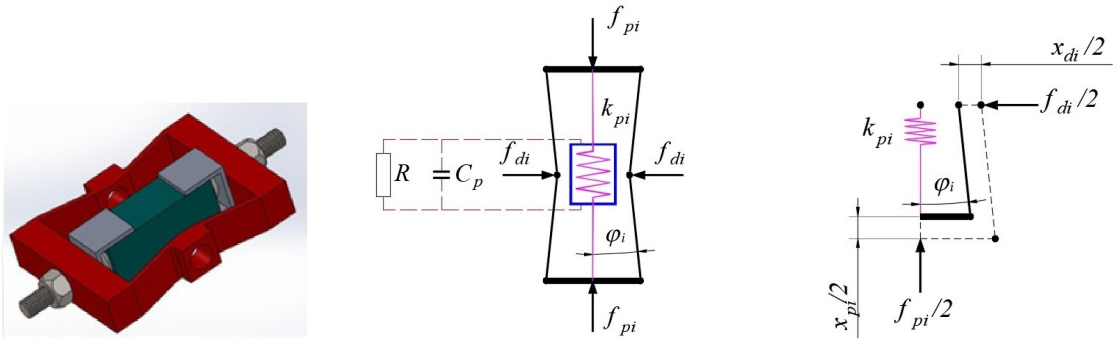

(a) Configuration (b) Physical model (c) Quarter free body

Fig. 1. Modeling 1sPSFAF

As depicted in Fig. 1(a), a single-stage PSFAF has only a FAF containing a piezo-stack, while the 2sPSFAF proposed in the Patent [11] consists of a primary FAF containing secondary single-stage PSFAFs which are assembled in series as seen in Fig. 2(a). For modeling this 2sPSFAF, one can first derive from the single-stage one which has been studied in [10, 12]. Assuming that each linkage of the FAF is an elastic element, has dismissed mass and hinge connections at both ends (no reaction moments) while other parts can be considered as a rigid body. Therefore, the deformations occurring in the linkages are so small that they are only axial. The force-voltage relationship of the piezo stack is governed by the following constitutive equations [10, 12, 13]

$$f_{p,i} = k_{p,i} x_{p,i} + \theta_{p,i} V_{p,i}\,, \tag{1}$$

$$q_i = \theta_{p,i} x_{p,i} - C_{p,i} V_{p,i}\,, \tag{2}$$

where $\theta_{p,i}$ is the effective electromechanical coupling coefficient, q_i is the produced electric charge, $C_{p,i}$ is the internal capacitance, and $V_{p,i}$ is the voltage of the PSEH caused by the axial force $f_{p,i}$ acting on the piezo stack. As proven in [10, 12] for the 1sPSFAF, the relationship between the input force and displacement, say $f_{d,i}$ and $x_{d,i}$, and the output ones, say $f_{p,i}$ and $x_{p,i}$, can be described by

$$\frac{x_{d,i}}{x_{p,i}} = \frac{f_{p,i}}{f_{d,i}} = \cot\varphi_i\,, \tag{3}$$

where φ_i is the structural angle of the single-stage FAF. Substituting (3) into (1) and (2), those constitutive equations can be rewritten in terms of $f_{d,i}$ and $x_{d,i}$ as follows

$$f_{d,i} = \frac{k_{p,i}}{\cot^2\varphi_i} x_{d,i} + \frac{\theta_{p,i}}{\cot\varphi_i} V_{p,i}\,, \tag{4}$$

$$q_i = \frac{\theta_{p,i}}{\cot\varphi_i} x_{d,i} - C_{p,i} V_{p,i}. \tag{5}$$

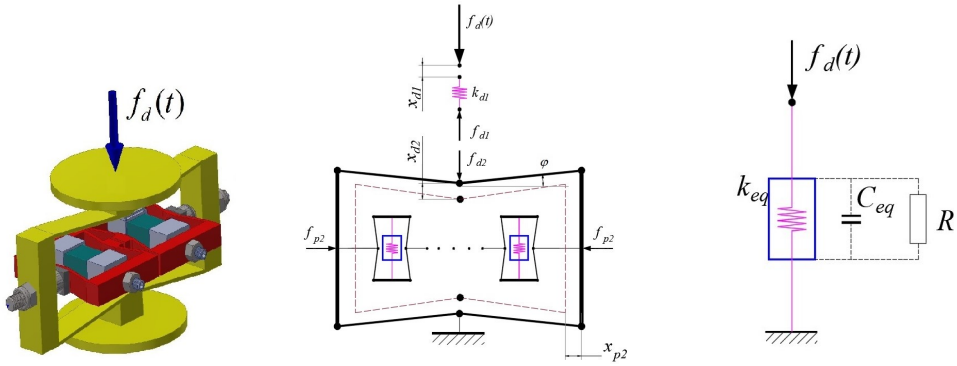

(a) Configuration (b) Physical model (c) Equivalent model

Fig. 2. Modeling a 2sPSFAF

Next, consider a 2sPSFAF with a primary FAF containing N elements of 1sPSFAF which are connected mechanically in series and electrically in parallel (see Fig. 2(b)). It is clear that

- Similar to the relationship (3), the relationship between the input force and displacement, say $f_{d,2}$ and $x_{d,2}$, and the output ones of the primary FAF with the structural angle φ, say $f_{p,2}$ and $x_{p,2}$, can be described by

$$\frac{x_{d,2}}{x_{p,2}} = \frac{f_{p,2}}{f_{d,2}} = \cot\varphi. \tag{6}$$

- The relationships between the output force and displacement of the primary FAF, $f_{p,2}$ and $x_{p,2}$, with that of the series combination of N elements of 1sPSFAF with the structural angle φ_i are, respectively

$$f_{p,2} = f_{d,i}, x_{p,2} = N x_{d,i}. \tag{7}$$

- The electrical quantities representing the parallel circuit of N capacitors, say the total electric discharge q, the total capacitance C_p, and the total voltage V_p, are, respectively

$$q = N q_i, C_p = N C_{p,i}, V_p = V_{p,i}. \tag{8}$$

Substituting (6) into (4) and (5) with noting (7), (8), those constitutive equations can be rewritten in terms of $f_{d,2}$ and $x_{d,2}$ as follows

$$f_{d,2} = \frac{k_{p,i}}{N\cot^2(\varphi_i)\cot(\varphi)} x_{d,2} + \frac{\theta_{p,i}}{\cot\varphi_i} V_p\,, \tag{9}$$

$$q = \frac{\theta_{p,i}}{\cot(\varphi_i)\cot(\varphi)} x_{d,2} - C_p V_p. \tag{10}$$

Rearranging (9) and (10) to get

$$f_{d,2} = k_{FAF} x_{d,2} + \theta_{FAF} V, \tag{11}$$

$$q = \theta_{FAF} x_{d,2} - C_p V, \tag{12}$$

where

$$k_{FAF} = \frac{k_{p,i}}{N\cot^2(\varphi_i)\cot(\varphi)}\,, \quad \theta_{FAF} = \frac{\theta_{p,i}}{\cot(\varphi_i)\cot(\varphi)}\,, \quad V = V_p\cot\varphi. \tag{13}$$

Thus, from the above modeling of single-stage and 2sPSFAFs, the following remarks could be drawn:

- The 1sPSFAF, which consists of a FAF containing a piezo stack, is equivalent to a PSEH governed by Eqs. (4), (5) which has been proven in [10,12].

- The proposed 2sPSFAF, which consists of a primary FAF containing 1sPSFAFs connected mechanically in series and electrically in parallel, is also equivalent to a PSEH governed by Eqs. (11)–(12).

2.2. Series combination of 2sPSFAF and a spring

Since the proposed 2sPSFAF can be modeled as an equivalent PSEH whose constitutive equations are given by (11)–(12), its series combination with a spring of stiffness k_d is governed by the following equations [10,12]

$$f_d = k_{eq} x_d + \theta_{eq} V, \tag{14}$$

$$q = \theta_{eq} x_d - C_{eq} V, \tag{15}$$

where

$$k_{eq} = \frac{k_d k_{FAF}}{k_d + k_{FAF}}\,, \quad \theta_{eq} = \frac{k_d}{k_d + k_{FAF}}\theta_{FAF}\,, \quad C_{eq} = C_p + \frac{\theta_{FAF}^2}{k_d + k_{FAF}}. \tag{16}$$

Substituting (13) into (16), one gets

$$\begin{gathered} k_{eq} = \frac{k_d k_{p,i}}{k_d N\cot^2(\varphi_i)\cot(\varphi) + k_{p,i}}\,, \quad \theta_{eq} = \frac{k_d N\cot(\varphi_i)}{k_d N\cot^2(\varphi_i)\cot(\varphi) + k_{p,i}}\theta_{p,i}\,, \\ C_{eq} = NC_{p,i} + \frac{N\cot(\varphi_i)}{k_d N\cot^2(\varphi_i)\cot(\varphi) + k_{p,i}}\theta_{p,i}^2. \end{gathered} \tag{17}$$

Once again, it is seen that the series combination of a spring and the proposed 2sPSFAF can be modeled as an equivalent PSEH where its constitutive equations (14)–(15) are expressed in the total deformation x_d and the applied force f_d of the combination.

2.3. A design consideration of TMD incorporating 2sPSFAF attached to undamped primary structure

The proposed system in the Patent [11] deals with a TMD incorporating a 2sPSFAF (TMD-2sPSFAF) which is depicted in Fig. 3(a). The primary structure has a mass m_s and a linear spring of stiffness k_s, it is undamped and subjected to harmonic external excitation $F(\bar{t})$

$$F(\bar{t}) = F_0 \cos \omega \bar{t}, \tag{18}$$

where $\bar{t}$ is the time, F_0 is amplitude, and ω is excitation frequency. The TMD-2sPSFAF has mass m_d, the linear viscous damper of damping coefficient c_d, the series combination of TMD's linear spring of stiffness k_d , and the 2sPSFAF. From the above proven, this series combination can be replaced by an equivalent PSEH as shown in Fig. 3(b). The equivalent PSEH has stiffness k_{eq}, effective electromechanical coupling coefficient θ_{eq}, and internal capacitance C_{eq}, which are given by (17). The free-body diagram in Fig. 3(c) represents the force balance of the masses where the force f_d of the equivalent PSEH is given by (14). Accordingly, the governing equations of the considered system are given by

$$\begin{aligned} &m_s\ddot{x}_s - c_d\dot{x}_d + k_s x_s - k_{eq}x_d - \theta_{eq}V = F_0\cos(\omega\bar{t}), \\ &m_d\ddot{x}_d + c_d\dot{x}_d + k_{eq}x_d + \theta_{eq}V = -m_d\ddot{x}_s\,, \\ &C_{eq}\dot{V} + \frac{V}{R} = \theta_{eq}\dot{x}_d\,, \end{aligned} \tag{19}$$

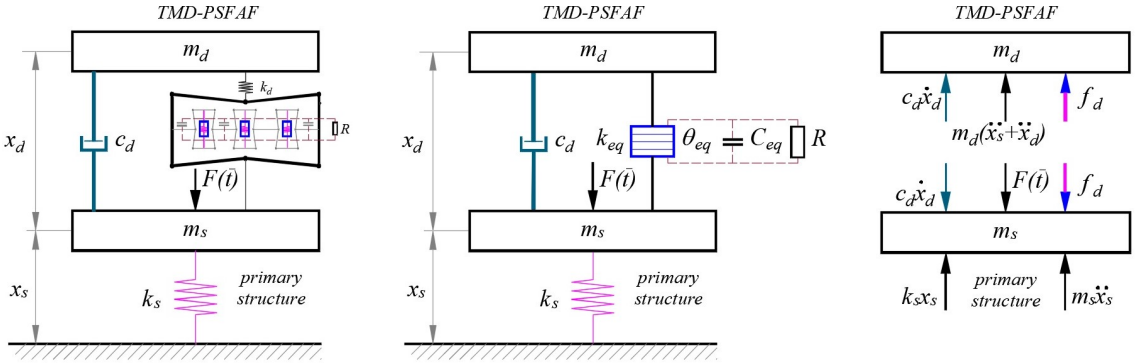

(a) Physical model (b) Equivalent model (c) Free-body diagram

Fig. 3. Undamped primary structure with TMD-2sPSFAF

where the third equation is obtained by integrating (15). Let us denote

$$t = \omega_s \bar{t},\ x_s = x_1,\ x_d = x_2,\ \omega_s = \sqrt{k_s/m_s},\ \omega_d = \sqrt{k_{eq}/m_d},\ \mu = m_d/m_s,$$
$$\xi_d = \frac{c_d}{2m_d\omega_d},\ \beta = \frac{\omega_d}{\omega_s},\ \lambda = \frac{\omega}{\omega_s},\ \kappa^2 = \frac{\theta_{eq}^2}{k_{eq}C_{eq}},\ v = \frac{C_{eq}V}{\theta_{eq}},\ \alpha = \frac{1}{\omega R C_{eq}},\ X_{st} = \frac{F_0}{k_s}. \tag{20}$$

Physically, ω_s and ω_d are the natural frequency of the primary structure and the equivalent PSEH, κ^2 is the electromechanical coupling coefficient, α is the resistance ratio, v is the transformed voltage, and $\mu, \xi_d, \beta, \lambda$ are the mass ratio, damping ratio, tuning ratio, and the ratio of excitation frequency to primary structure frequency, respectively. The equation system (19) can be transformed into the following dimensionless system

$$\begin{aligned}
&\ddot{x}_1 - 2\mu\beta\xi_d\dot{x}_2 + x_1 - \mu\beta^2 x_2 - \mu\beta^2\kappa^2 v = X_{st}\cos\lambda t,\\
&\ddot{x}_2 + 2\beta\xi_d\dot{x}_2 + \beta^2 x_2 + \beta^2\kappa^2 v = -\ddot{x}_1\,,\\
&\dot{v} + \lambda\alpha v = \dot{x}_2\,,
\end{aligned} \tag{21}$$

where the over dots now denote the derivatives regarding dimensionless time t. It is seen that the system (21) is a linear system of ordinary differential equations for three unknowns, $x_1(t), x_2(t)$ and $v(t)$, which can be analytically solved.

It is seen from (21) that when $\kappa^2 = 0$ one gets the corresponding mechanical TMD system. Normally, κ^2 has a small value for various piezo materials. Hence, to investigate the undamped primary structure with TMD-2sPSFAF in considering $\kappa^2 \to 0$, the results of the optimal mechanical TMD obtained by the fixed point theory [15, 16] are adopted for β and ξ_d of TMD-2sPSFAF

$$\beta = \frac{\omega_d}{\omega_s} = \sqrt{\frac{1}{\mu}\frac{k_{eq}}{k_s}} = \frac{1}{1+\mu}, \tag{22}$$

$$\xi_d = \sqrt{\frac{3\mu}{8(1+\mu)}}. \tag{23}$$

From (22) one has

$$k_{eq} = \frac{\mu}{(1+\mu)^2}k_s. \tag{24}$$

Substituting (24) into the first equation in (17), one gets

$$k_d = \frac{\mu k_s k_{p,i}}{(1+\mu)^2 k_{p,i} - \mu N\cot^2(\varphi_i)\cot(\varphi)k_s}. \tag{25}$$

Clearly, the number N of 1sPSFAFs should be a positive integer. Since φ_i, φ are normally small angles, say $\varphi_i, \varphi < 10^\circ$ [8,9] then $\cot\varphi, \cot\varphi_i > 0$. Hence, to ensure k_d being

positive, the following condition is extracted from (25)

$$\begin{aligned} &(1+\mu)^2 k_{p,i} - \mu N \cot^2(\varphi_i)\cot(\varphi) k_s > 0 \\ \Leftrightarrow\ &\frac{k_{p,i}}{k_s} > \frac{\mu N \cot^2(\varphi_i)\cot(\varphi)}{(1+\mu)^2}. \end{aligned} \tag{26}$$

From a technical perspective, the mass ratio μ and the primary structure stiffness k_s are known. The characteristic parameters of FAFs, such as structural angles φ_i, φ, as well as that of PSEHs, such as the stiffness $k_{p,i}$, the effective electromechanical coupling coefficient $\theta_{p,i}$, and the internal capacitance $C_{p,i}$, can be chosen from available materials. Thus, (26) provides the condition for choosing stiffness $k_{p,i}$, then the stiffness of TMD's spring k_d could be obtained by (25).

It is interesting to see from (25) that we can generalize cases of TMD-PSEH with FAFs. Namely, when $\cot\varphi = 1$, one obtains

$$k_d = \frac{\mu k_s k_{p,i}}{(1+\mu)^2 k_{p,i} - \mu N \cot^2(\varphi_i) k_s}, \tag{27}$$

which is the case of the TMD-1sPSFAF system as studied in [13]. When $\cot\varphi = \cot\varphi_i = 1$, one obtains

$$k_d = \frac{\mu k_s k_{p,i}}{(1+\mu)^2 k_{p,i} - \mu N k_s}, \tag{28}$$

which is the case of TMD-PSEH without FAF as studied in [14].

3. NUMERICAL EXAMINATION

In this section, we carry out a numerical investigation of the undamped primary structure-TMD-2sPSFAF system. The proposed design procedure for a given system will follow that presented in Section 2. The initial input parameters are taken as presented in Table 1 and Table 2. The calculated parameters used for investigation are presented in Table 3.

Table 1. Physical properties of a piezo stack [7]

Parameter	Symbol	Value	Unit
Stiffness	$k_{p,i}$	5.8×10^7	N/m
Effective electromechanical coupling coefficient	$\theta_{p,i}$	8.41	N/V
Capacitance	$C_{p,i}$	1.6×10^{-6}	F

Fig. 4(a) and Fig. 4(b) depict the curves of the mechanical magnification factor K_1 and the voltage amplitude factor v_0 in the frequency domain λ, respectively.

Table 2. Initial input parameters

Parameter	Symbol	Value	Unit
Mass ratio	μ	0.05	
Primary structure stiffness	k_s	1% $k_{p,i}$	N/m
Structural angle of primary FAF [9]	φ	$\pi/30$	rad
Structural angle of single-stage FAF [9]	φ_i	$\pi/30$	rad
Number elements of 1sPSFAF	N	2	
Electrical resistance ratio	α	1	

Table 3. Calculated parameters used for investigation

Parameter	Value	Referenced Eqs.	Parameter	Value	Referenced Eqs.
k_d (N/m)	1.2022×10^5	(25)	C_{eq} (F)	8.28×10^{-6}	(17)
k_{eq} (N/m)	2.6304×10^4	(17)	β	0.9524	(22)
θ_{eq} (N/V)	0.0726	(17)	κ^2	0.0242	(20)

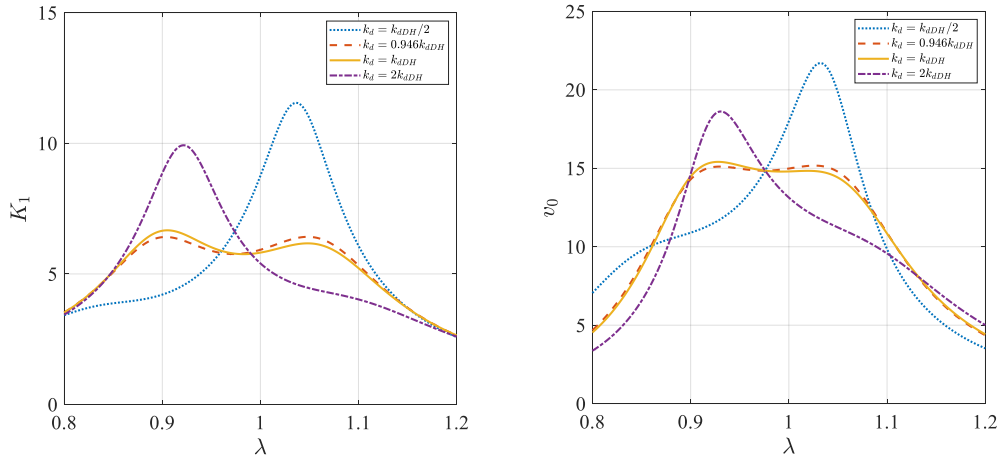

(a) K_1 (b) v_0

Fig. 4. K_1, v_0 versus λ with $\mu = 0.05, \kappa^2 = 0.0242, \alpha = 1$ and k_d varies

The effect of the TMD spring stiffness k_d on K_1 is illustrated in Fig. 4(a) with four different values of k_d, where k_{dDH} is given by Eq. (25). It is seen that the curve K_1 always has two peaks, however, it is not optimized due to the heights of those two peaks are not equal in the case $k_d = k_{dDH}/2$, $k_d = k_{dDH}$, and $k_d = 2k_{dDH}$. Thus, the optimal tuning and damping coefficients given by Eqs. (22), (23) derived from Den Hartog's result do not ensure the curve K_1 being optimized. Meanwhile, we can optimize K_1 by changing

the value of k_d empirically, say $k_d = 0.946k_{dDH}$ that is a little smaller than k_{dDH}. Consequently, the coordinates of the corresponding left and right peaks are $(0.904; 6.414)$ and $(1.052; 6.414)$, respectively.

At the first glance, the curve v_0 has the same properties as that of the curve K_1, as shown in Fig. 4(b). With the value $k_d = 0.946k_{dDH}$, the curve v_0 is almost optimized, namely the two peaks are equal with coordinates of $(0.927; 15.11)$ and $(1.034; 15.14)$, respectively. Furthermore, it is seen that the curve v_0 has a fixed point independent of the TMD spring stiffness k_d. Therefore, one can see a good matching between the mechanical domain and the electrical one with the effective value of k_d, i.e. $k_d = 0.946k_{dDH}$.

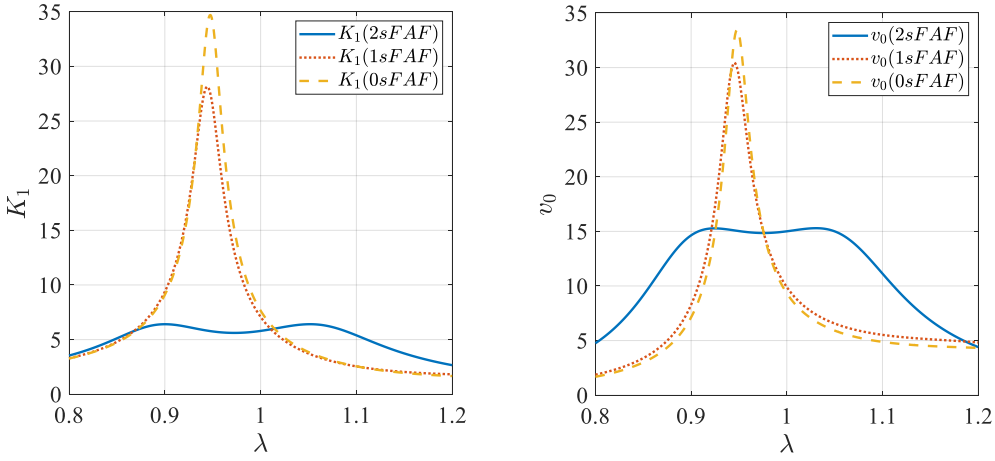

(a) K_1 (b) v_0

Fig. 5. K_1, v_0 versus λ with $\mu = 0.05, \kappa^2 = 0.0242, \alpha = 1, k_d = 0.946k_{dDH}$ in cases of with and without FAF

To compare the performance of the TMD-PSEH system in the cases with FAFs (2sPSFAF, 1sPSFAF) and without FAF (0sPSFAF), the corresponding TMD spring stiffnesses given by (25), (27), (28) are used. The plots of K_1 and v_0 are depicted in Fig. 5(a) and Fig. 5(b), respectively, with the number of 1sPSFAFs $N = 1$. Clearly, there are differences in the TMD spring's equivalent stiffness between these three scenarios, namely $k_{eq-0sPSEH} = 4.292 > k_{eq-1sFAF} = 4.025 > k_{eq-2sPSFAF} = 2.622$. As a result, the equivalent stiffness of the softer TMD spring results in less vibration of the primary structure (see Fig. 5(a)). Meanwhile, although the peak voltage amplitude of the 2sPSFAF case may be lower than the other two cases, in return it changes little over the entire resonant frequency domain as seen in Fig. 5(b). As discussed in [14], the design of 2sPSFAF ensures the priority of vibration suppression for the piezo TMD system but still allows a large enough voltage in the resonant domain.

4. CONCLUSION

Key works and findings included in the article are as follows:

- A novel configuration for a piezo TMD is introduced, in which the springs of the TMD are coupled in series with the two-stage force amplification frames (FAFs) and piezo stacks.

- After establishing the constitutive equations of 2sPSFAF, it is demonstrated that the reduced order model of the 2sPSFAF and TMD spring series combination is an analogous piezo stack energy harvester. The TMD-2sPSFAF system's governing equations, which include three responses for mechanical and electrical variables, are then executed.

- The fixed point theory ideal results are used to determine the requirements for choosing the TMD spring and piezo stack stiffnesses.

- Subsequently, a computational analysis of the electromechanical system shows that the voltage amplitude curve has a fixed point that is unaffected by the stiffness of the TMD spring. In addition, the TMD spring's effective stiffness would be determined to guarantee that the voltage amplitude and mechanical magnification curve peaks are at the same heights.

- Taking into consideration all these facts, the optimal design of TMD-PSEH with multi-FAFs should be further developed.

DECLARATION OF COMPETING INTEREST

The authors declare that they have no known competing financial interests or personal relationships that could have appeared to influence the work reported in this paper.

FUNDING

This research received no specific grant from any funding agency in the public, commercial, or not-for-profit sectors.

REFERENCES

[1] A. Erturk and D. J. Inman. *Piezoelectric energy harvesting*. Wiley, (2011). https://doi.org/10.1002/9781119991151.

[2] M. Goldfarb and N. Celanovic. Modeling piezoelectric stack actuators for control of micromanipulation. *IEEE Control Systems Magazine*, **17**, (3), (1997), pp. 69–79.

[3] F. Qian, T.-B. Xu, and L. Zuo. Design, optimization, modeling and testing of a piezoelectric footwear energy harvester. *Energy Conversion and Management*, **171**, (2018), pp. 1352–1364. https://doi.org/10.1016/j.enconman.2018.06.069.

[4] X. Jiang, Y. Li, J. Li, J. Wang, and J. Yao. Piezoelectric energy harvesting from traffic-induced pavement vibrations. *Journal of Renewable and Sustainable Energy*, **6**, (2014). https://doi.org/10.1063/1.4891169.

[5] W. Hendrowati, H. L. Guntur, and I. N. Sutantra. Design, modeling and analysis of implementing a multilayer piezoelectric vibration energy harvesting mechanism in the vehicle suspension. *Engineering*, **04**, (11), (2012), pp. 728–738. https://doi.org/10.4236/eng.2012.411094.

[6] J. Wang, Z. Shi, H. Xiang, and G. Song. Modeling on energy harvesting from a railway system using piezoelectric transducers. *Smart Materials and Structures*, **24**, (2015), p. 105017. https://doi.org/10.1088/0964-1726/24/10/105017.

[7] Y.-A. Lai, J.-Y. Kim, C.-S. W. Yang, and L.-L. Chung. A low-cost and efficient d33-mode piezoelectric tuned mass damper with simultaneously optimized electrical and mechanical tuning. *Journal of Intelligent Material Systems and Structures*, **32**, (2020), pp. 678–696. https://doi.org/10.1177/1045389x20966056.

[8] Y. Wang, W. Chen, and P. Guzman. Piezoelectric stack energy harvesting with a force amplification frame: Modeling and experiment. *Journal of Intelligent Material Systems and Structures*, **27**, (2016), pp. 2324–2332. https://doi.org/10.1177/1045389x16629568.

[9] L. Wang, S. Chen, W. Zhou, T.-B. Xu, and L. Zuo. Piezoelectric vibration energy harvester with two-stage force amplification. *Journal of Intelligent Material Systems and Structures*, **28**, (2016), pp. 1175–1187. https://doi.org/10.1177/1045389x16667551.

[10] N. N. Linh, V. A. Tuan, N. V. Tuan, and N. D. Anh. Response analysis of undamped primary system subjected to base excitation with a dynamic vibration absorber integrated with a piezoelectric stack energy harvester. *Vietnam Journal of Mechanics*, **44**, (2022), pp. 490–499. https://doi.org/10.15625/0866-7136/17948.

[11] N. N. Linh, N. D. Anh, L. D. Viet, N. A. Ngoc, V. A. Tuan, T. D. Nang, and N. V. Manh. *Patent Title: Tuned mass damper with integrated vibrating piezoelectric energy harvester*. Intellectual Property Office of Vietnam, Patent number: 39054, Application Number: 1-2022-02620, Publication Number: 1/088043 A, Publication date: 26 July (in Vietnamese), (2024). https://ipvietnam.gov.vn/documents/20182/1630076/39054.pdf/c254ef2a-e0ac-491f-ba4c-6709cda1b0a2.

[12] N. N. Linh. Series combination models of piezoelectric energy harvesters with spring and damper. In *the 11th National Conference on Mechanics*, Vol. 2, (2022).

[13] N. N. Linh and N. D. Anh. A novel configuration of tuned mass damper with energy harvester of piezoelectric stack and force amplification frame. In *Proceedings of the 7th International Conference on Engineering Mechanics and Automation*, Publishing House for Science and Technology, ICEMA 2023, (2023). https://doi.org/10.15625/vap.2023.0146.

[14] N. D. Anh, V. A. Tuan, P. M. Thang, and N. N. Linh. Extension of the fixed point theory to tuned mass dampers with piezoelectric stack energy harvester. *Journal of Sound and Vibration*, **581**, (2024). https://doi.org/10.1016/j.jsv.2024.118411.

[15] J. D. Hartog. *Mechanical vibrations*. Dover, New York, (1985).

[16] J. Connor and S. Laflamme. *Structural motion engineering*. Springer International Publishing, Switzerland, (2014).